

2-Aminoimidazole Amino Acids as Inhibitors of the Binuclear Manganese Metalloenzyme Human Arginase I

Monica Ilies,[†] Luigi Di Costanzo,^{†,§} Michelle L. North,[‡] Jeremy A. Scott,[‡] and David W. Christianson^{*,†}

[†]Roy and Diana Vagelos Laboratories, Department of Chemistry, University of Pennsylvania, Philadelphia, Pennsylvania 19104-6323, and
[‡]Department of Medicine, Faculty of Medicine, Divisions of Occupational and Respiratory Medicine, University of Toronto, Toronto, Ontario, M5S 1A8, Canada. [§]Present address: RCSB Protein Data Bank, Department of Chemistry and Chemical Biology, Rutgers, The State University of New Jersey, Piscataway, New Jersey 08854-8087.

Received March 8, 2010

Arginase, a key metalloenzyme of the urea cycle that converts L-arginine into L-ornithine and urea, is presently considered a pharmaceutical target for the management of diseases associated with aberrant L-arginine homeostasis, such as asthma, cardiovascular diseases, and erectile dysfunction. We now report the design, synthesis, and evaluation of a series of 2-aminoimidazole amino acid inhibitors in which the 2-aminoimidazole moiety serves as a guanidine mimetic. These compounds represent a new class of arginase inhibitors. The most potent inhibitor identified in this study, 2-(*S*)-amino-5-(2-aminoimidazol-1-yl)pentanoic acid (A1P, **10**), binds to human arginase I with $K_d = 2 \mu\text{M}$ and significantly attenuates airways hyperresponsiveness in a murine model of allergic airways inflammation. These findings suggest that 2-aminoimidazole amino acids represent new leads for the development of arginase inhibitors with promising pharmacological profiles.

Introduction

Arginase is a metalloenzyme that catalyzes the hydrolysis of L-arginine to form L-ornithine and urea. Two distinct isozymes with different tissue distributions, subcellular localizations, and metabolic functions have been identified in mammals.¹ The cytosolic isozyme, arginase I, is found mainly in the liver where it catalyzes the final cytosolic step of the urea cycle. Here, arginase activity allows for the ultimate excretion of excess nitrogen resulting from protein catabolism in the form of urea.² The mitochondrial isozyme, arginase II, is predominantly expressed in extrahepatic tissues³ where it serves to regulate L-arginine homeostasis and biosynthetic pathways dependent on L-arginine and L-ornithine. These pathways include nitric oxide (NO^o) biosynthesis, L-proline biosynthesis to support collagen production (as an alternative to the L-glutamate derived biosynthesis of L-proline), and polyamine biosynthesis to facilitate cellular proliferation (Figure 1).^{4–6} Arginase I is also expressed in extrahepatic tissues to regulate L-arginine homeostasis.⁷ For example, arginase I expression is significantly increased in the asthmatic lung.⁸ Arginase I is more strongly induced by Th2 cytokines such as IL-13 that have a critical role in the development of asthma in experimental models,⁹ while arginase I and II single-nucleotide polymorphisms may contribute to atopic asthma.¹⁰ Additionally,

arginase inhibition or posttranscriptional gene silencing of arginase I significantly decreases airways hyperresponsiveness induced by IL-13 or aeroallergens in different animal models.¹¹ The role of arginase in asthma has been recently reviewed.¹² In addition to asthma, the biochemical interplay between arginase and nitric oxide synthase makes arginase an increasingly important pharmaceutical target for the management of various diseases associated with aberrant L-arginine homeostasis and/or NO biosynthesis, such as erectile dysfunction,^{13,14} pulmonary diseases such as cystic fibrosis,¹⁵ cardiovascular diseases including atherosclerosis,¹⁶ and cancer tumor growth.¹⁷

In the active site of arginase, the binuclear manganese cluster and residues that interact with the α -amino and α -carboxylate groups of amino acid inhibitors constitute essential molecular recognition elements for high affinity binding. X-ray crystallographic studies of rat arginase I and human arginase I complexed with inhibitors such as 2-(*S*)-amino-6-borohexanoic acid (ABH)^{13a,18,19} and *S*-(2-boronoethyl)-L-cysteine (BEC)^{13b,19} serve to guide continuing studies toward the structure-based design of new inhibitors that bear alternative functional groups targeting coordination interactions with the binuclear manganese cluster. New inhibitors with different chemical properties may exhibit alternative pharmacokinetic profiles that enable their study as potential lead compounds for drug development.

We have previously shown that the guanidine side chain of L-arginine is not a particularly effective metal ligand.²⁰ The positively charged guanidinium group has a high pK_a value of 12.5–13,²¹ so protonation significantly competes with potential metal coordination behavior. However, the incorporation of a guanidinium group within a 2-aminoimidazole heterocycle reduces the pK_a by 4–5 units,²² which in turn can facilitate metal coordination interactions and improve the

*To whom correspondence should be addressed. Phone: 215-898-5714. Fax: 215-573-2201. E-mail: chris@sas.upenn.edu.

^oAbbreviations: SAR, structure–activity relationship; NO, nitric oxide; ABH, 2-(*S*)-amino-6-borohexanoic acid; BEC, *S*-(2-boronoethyl)-L-cysteine; 2AH, L-2-aminohistidine; AHH, 2-aminohomohistidine; A1P, 2-(*S*)-amino-5-(2-aminoimidazol-1-yl)pentanoic acid; A4P, 2-amino-5-(2-aminoimidazol-4-yl)pentanoic acid; APP, (*S*)-2-amino-5-(imidazol-2-ylamino)pentanoic acid; DIBAH, diisobutylaluminum hydride; DMAP, dimethylaminopyridine; DMF, dimethylformamide; TFA, trifluoroacetic acid.

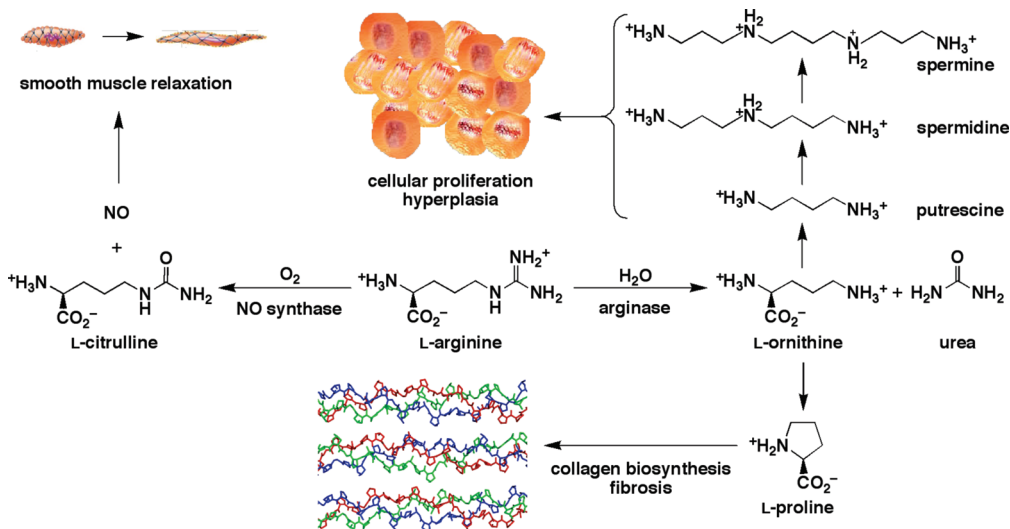


Figure 1. Pathways of L-arginine metabolism.

pharmacokinetic profile. Accordingly, 2-aminoimidazole derivatives display a broad range of biological properties and represent significant precursors for drug design and natural products synthesis. Interestingly, 2-aminoimidazoles have been isolated from marine sponges as secondary metabolites known as oroidins, which exhibit a wide range of biological activities.^{23–25}

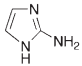
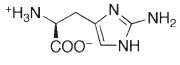
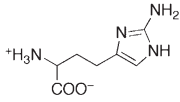
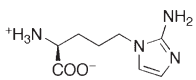
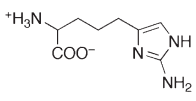
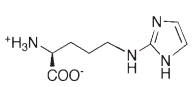
Although certain 2-aminoimidazole amino acids have been reported with potential applications in medicinal chemistry,^{26–28} such compounds have never been investigated as arginase inhibitors. Here, we report the structure-based design, synthesis, and evaluation of a series of 2-aminoimidazole amino acid inhibitors of human arginase I. The most active of these compounds, 2-(*S*)-amino-5-(2-aminoimidazol-1-yl)pentanoic acid (A1P, **10**), binds to human arginase I with low micromolar affinity and significantly reduces airways hyperresponsiveness in a murine model of allergic airways inflammation. On the basis of these findings, we advance that 2-aminoimidazole amino acids may serve as valuable leads for the development of a new class of arginase-directed drugs. Moreover, the utilization of a 2-aminoimidazole moiety to target metal coordination interactions is potentially generalizable toward the inhibition of other binuclear metallohydrolases.

Results

Chemistry and in Vitro Structure–Activity Relationships (SARs). 2-Aminoimidazole (Table 1) is a weak noncompetitive inhibitor of human arginase I with $K_i = 3.6$ mM. The X-ray crystal structure of the enzyme–inhibitor complex (Figure 2) reveals that 2-aminoimidazole binds in the active site but does not interact directly with the binuclear manganese cluster. Instead, the inhibitor is aligned parallel to the imidazole group of H126 with a mean interplane distance of ~ 4 Å. Additionally, the 2-amino group donates a hydrogen bond to a water molecule that in turn donates a hydrogen bond to the metal-bridging hydroxide ion. In studying the structure of this complex, we reasoned that the 2-aminoimidazole moiety could be targeted to interact directly with the binuclear manganese cluster by incorporating it within the side chain of an L-amino acid.

The synthesis of the simplest member of the series of 2-aminoimidazole amino acids shown in Table 1, L-2-amino-histidine (2AH), was achieved using a previously published procedure.²⁶ This compound exhibits noncompetitive

Table 1. 2-Aminoimidazole and Amino Acid Derivatives Synthesized as Inhibitors of Human Arginase I

Compound	K_i (μM) ^a
2-Aminoimidazole	
	3600 ± 20
2AH	
	300 ± 9
AHH	
	3000 ± 10
A1P	
	4.0 ± 0.2
A4P	
	> 800000
APP	
	500 ± 8

^a Kinetic assay. Errors are standard deviations of experiments run in triplicate. ^b Surface plasmon resonance measurement of the dissociation constant, K_d .

inhibition against human arginase I with a ~ 10 -fold increase in inhibitor binding affinity ($K_i = 0.3$ mM) relative to 2-aminoimidazole.

The X-ray crystal structure of the human arginase I–2AH complex (Figure 3) reveals that the 2-aminoimidazole group

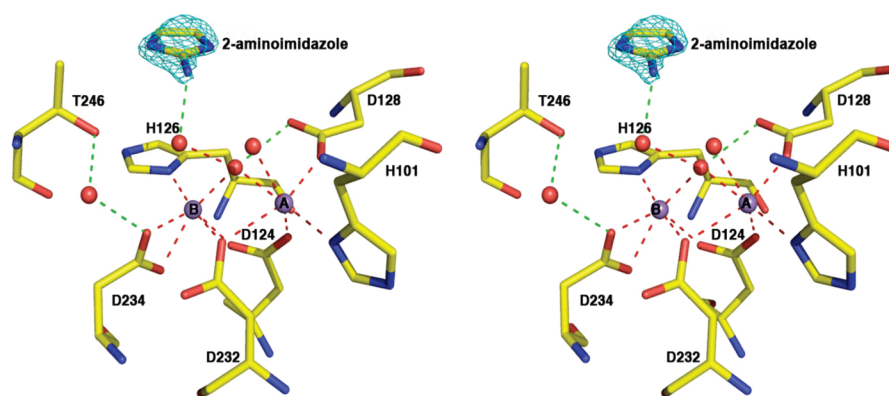


Figure 2. Stereoview of a simulated annealing gradient map showing 2-aminoimidazole (3.0σ contour, cyan) bound to human arginase I. Dashed lines indicate manganese coordination (red) and hydrogen bond (green) interactions. Atom color codes are as follows: carbon (yellow), oxygen (red), nitrogen (blue), manganese (violet).

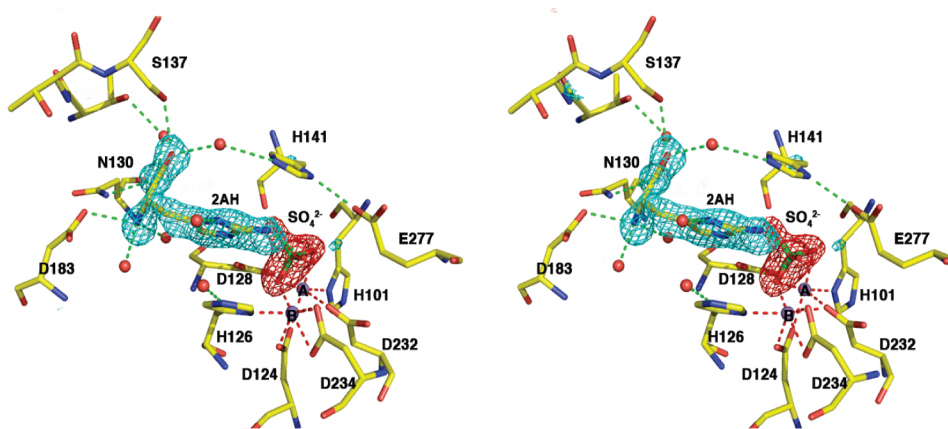


Figure 3. Stereoview of a simulated annealing omit map showing the inhibitor 2AH and a sulfate ion bound to human arginase I. The inhibitor (3.0σ contour, cyan) and sulfate ion (3.5σ contour, red) were omitted from the structure factor calculation. The sulfate ion coordinates to the manganese ions and accepts hydrogen bonds from the side chain of 2AH. Dashed lines indicate manganese coordination (red) and hydrogen bond (green) interactions. Atom color codes are as follows: carbon (yellow), oxygen (red), nitrogen (blue), manganese (violet), sulfur (green).

is repositioned in the active site, but the side chain is too short to interact directly with the binuclear manganese cluster. However, inhibitor binding recruits a tetrahedral anion interpreted as sulfate to achieve manganese coordination. As observed for the binding of other amino acid inhibitors,^{19,29} the α -amino group donates hydrogen bonds to D183 and two water molecules, and the α -carboxylate group accepts hydrogen bonds from N130, S137, and two water molecules (Figure 3). Hydrogen bond interactions between the 2-aminoimidazole group and the metal-bound sulfate anion stabilize inhibitor binding and may contribute to the ~ 10 -fold increase in affinity relative to 2-aminoimidazole. Although the binding affinity of 2AH is modest, the intermolecular interactions observed in the human arginase I–2AH complex illuminate a novel coordination mode to the binuclear manganese cluster.

Given that the side chain of 2AH is too short to allow the 2-aminoimidazole group to interact directly with the manganese ions, we synthesized the congener 2-aminohomohistidine (AHH, Table 1), which bears a side chain one carbon longer, using a previously published procedure.²⁷ AHH is a competitive inhibitor with $K_i = 3$ mM for the racemic mixture, indicating no significant improvement in the binding affinity compared with 2AH.

The X-ray crystal structure of the human arginase I–AHH complex (Figure 4) reveals that the α -amino and α -carboxylate groups make the expected hydrogen bond

interactions in the active site as observed for the binding of other amino acid inhibitors.^{19,29} Additionally, the 2-aminoimidazole group of AHH displaces the metal-bridging hydroxide ion of the unliganded enzyme and coordinates to Mn^{2+}_A with an average $\text{N}\cdots\text{Mn}^{2+}_A$ separation of 2.5 Å. The $\text{N}\cdots\text{Mn}^{2+}_B$ separation is 2.8 Å, which is too long to be considered an inner sphere coordination interaction. The imidazole group of AHH is sandwiched between the imidazole groups of H126 and H141 with mean interplane separations of 3.5 and 3.6 Å, respectively. The lengthy metal coordination interactions observed in this enzyme–inhibitor complex, which should be closer to 2.0 Å for optimal $\text{N}\cdots\text{Mn}^{2+}$ interactions, may be responsible for the lower binding affinity of AHH.

Encouraged by these structural results, we opted to investigate three different derivatives bearing aminoimidazole side chains one carbon longer than that of AHH: 2-(*S*)-amino-5-(2-aminoimidazol-1-yl)pentanoic acid (A1P), 2-amino-5-(2-aminoimidazol-4-yl)pentanoic acid (A4P), and (*S*)-2-amino-5-(imidazol-2-ylamino)pentanoic acid (APP) (Table 1). We used the protected *L*-amino acid aldehyde **4** and the triprotected 2-aminoimidazole **5** as key intermediates in the syntheses of these derivatives (Scheme 1).

The aldehyde **4** was synthesized from commercially available (*S*)-5-*tert*-butoxy-4-(*tert*-butoxycarbonylamino)-5-oxopentanoic acid (**1**) that was first esterified with methyl

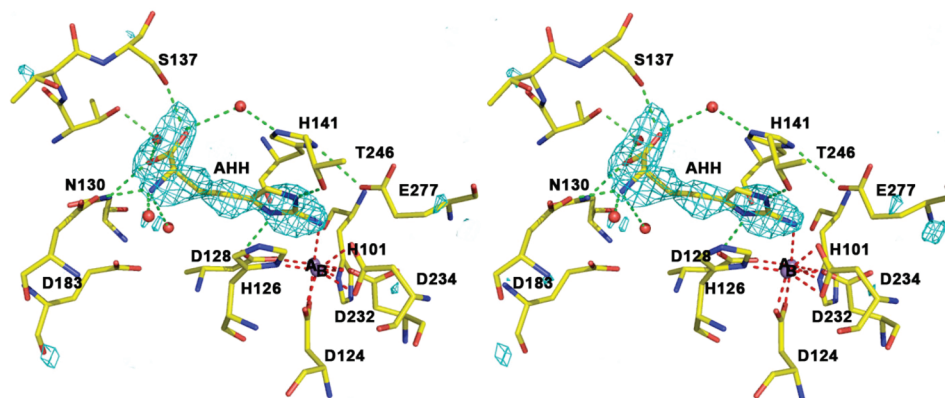
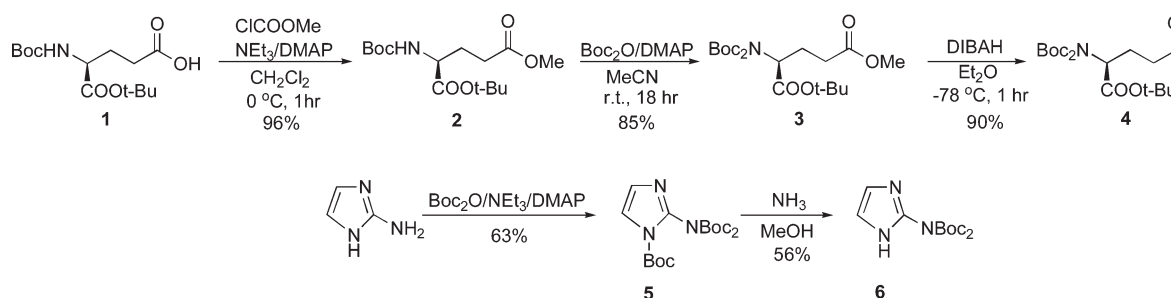
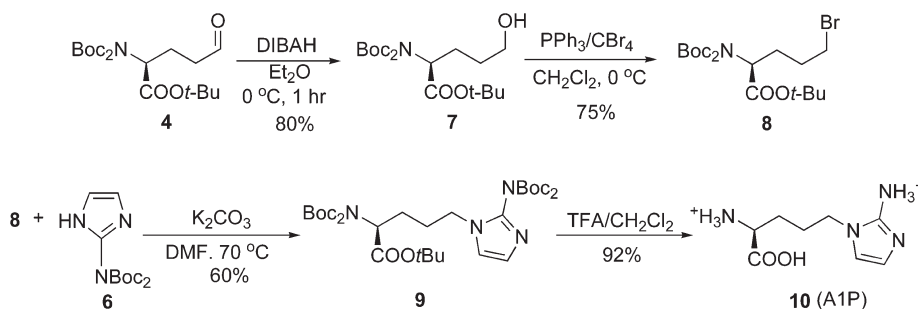


Figure 4. Stereoview of a simulated annealing omit map showing the inhibitor AHH bound to human arginase I. The inhibitor (3.0σ contour, cyan) was omitted from the structure factor calculation. Dashed lines indicate manganese coordination (red) and hydrogen bond (green) interactions. Atom color codes are as follows: carbon (yellow), oxygen (red), nitrogen (blue), manganese (violet).

Scheme 1. Synthesis of the Key Intermediates 4 and 6



Scheme 2. Synthesis of A1P



chloroformate, then further N-protected with a second *tert*-butoxycarbonyl group (intermediates **2** and **3**, respectively). Selective reduction of the less sterically hindered methyl ester group of **3** with diisobutylaluminum hydride (DIBAH) at $-78\text{ }^{\circ}\text{C}$ provided the corresponding aldehyde **4** in good overall yield.³⁰ The heterocyclic intermediates were generated by the treatment of 2-aminoimidazole with di-*tert*-butyl pyrocarbonate, yielding the derivative **5** that was selectively deprotected with ammonia in methanol to form 2-[bis(*tert*-butoxycarbonyl)amino]imidazole (**6**).

While the synthesis of A1P has been previously reported,³¹ we developed an alternative synthetic route with a comparable overall yield. We reduced the aldehyde intermediate **4** with DIBAH to form alcohol **7** (Scheme 2). Bromination of **7** with triphenylphosphine and carbon tetrabromide led to the corresponding bromo derivative **8** (as previously reported by our group³²), which was then coupled to the selectively protected 2-aminoimidazole **6** with potassium carbonate in dimethylformamide (DMF) to yield protected A1P (**9**); complete deprotection with trifluoroacetic acid

(TFA) in methylene chloride generated A1P (**10**) in good overall yield. While it is conceivable that racemization of the amino acid could occur under these conditions, racemization of a related amino acid was blocked by the utilization of a bulky *tert*-butyl protecting group on the α -carboxylate,³³ as we have similarly utilized for the preparation of A1P.

Two different assays indicate that A1P binds to human arginase I with low micromolar affinity. The fixed-point kinetic assay using ^{14}C -labeled L-arginine³⁴ demonstrates that A1P is a competitive inhibitor with $K_i = 4\text{ }\mu\text{M}$ (Figure 5A). Surface plasmon resonance analysis³⁵ confirms low micromolar affinity with $K_d = 2\text{ }\mu\text{M}$ in a 1:1 Langmuir binding model (Figure 5B). Unfortunately, we were unable to prepare crystals of human arginase I complexed with A1P by crystal soaking or cocrystallization approaches.

The N-alkylated derivative (APP, **12**) was synthesized by the reductive coupling of aldehyde intermediate **4** with 2-aminoimidazole to yield protected APP (**11**); deprotection with TFA in methylene chloride generated APP (**12**) (Scheme 3).

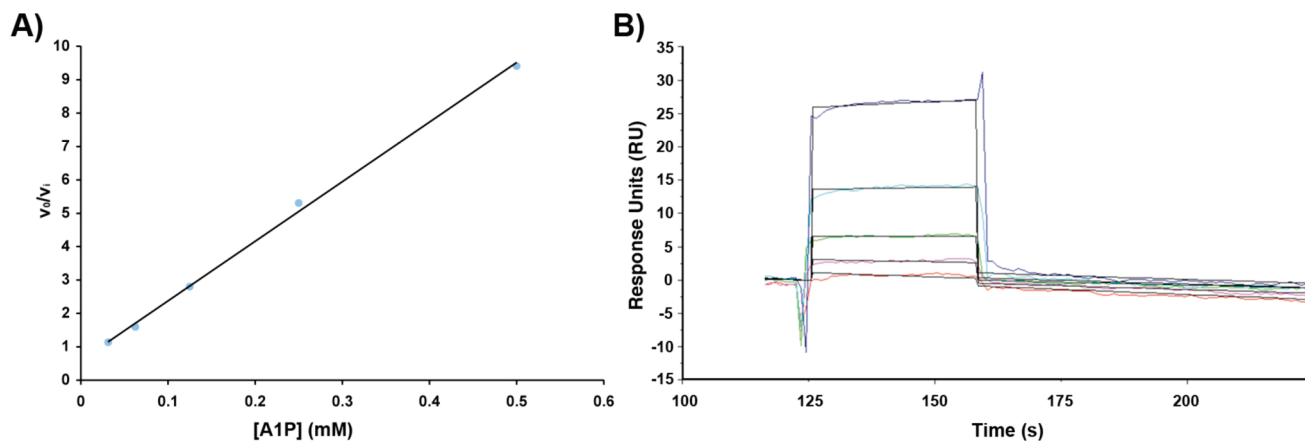
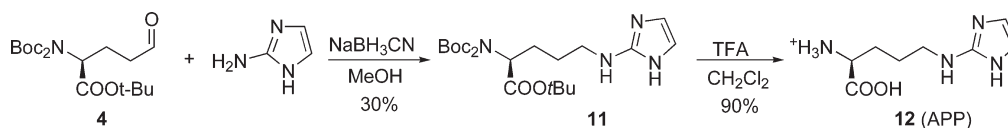
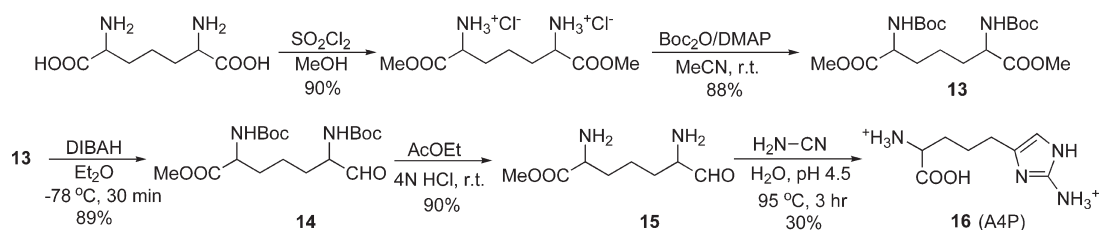


Figure 5. (A) Kinetic replot of the inhibition of human arginase I by A1P yields $K_i = 4 \mu\text{M}$. (B) Surface plasmon resonance sensorgram showing the binding of A1P to human arginase I; $K_d = 2 \mu\text{M}$.

Scheme 3. Synthesis of APP



Scheme 4. Synthesis of A4P



Enzymological measurements indicate that APP binds to human arginase I with modest affinity ($K_i = 500 \mu\text{M}$, Table 1). Alkylation via the 2-amino group increases the length of the amino acid side chain, which may contribute to decreased affinity relative to A1P.

The synthesis of A4P (Scheme 4) started from the commercially available 2,6-diaminoheptanedioic acid, which was diesterified with thionyl chloride in methanol, then N-protected with di-*tert*-butyl pyrocarbonate in acetonitrile in the presence of dimethylaminopyridine (DMAP) to generate the protected intermediate **13**. One ester group of **13** was then selectively reduced to the corresponding aldehyde **14** by using 1 equiv of DIBAL. Deprotection with 4 N HCl and ethyl acetate (EtOAc) generated the diaminoaldehyde **15** that was condensed with cyanamide in water³⁶ at pH 4.5 to afford A4P (**16**). Enzymological assay indicates that A4P lacks inhibitory activity ($K_i > 0.8 \text{ M}$).

Arginase Inhibition by A1P in a Murine Model of Allergic Airways Inflammation. To determine the effectiveness of the tightest binding 2-aminoimidazole amino acid, A1P, for reducing airways hyperresponsiveness *in vivo*, we used an acute (3-week) ovalbumin (OVA)-sensitization and -challenge murine model, as previously described.^{8a} In this model, mice sensitized with OVA but challenged with PBS (OVA/PBS) serve as controls, while OVA-sensitized and -challenged mice (OVA/OVA) develop lung-specific airways inflammation and airways hyperresponsiveness, as a model of asthma. We have previously shown that pharmacologic

inhibition of arginase with BEC attenuates maximum central airways responsiveness ($R_{N\text{max}}$) to methacholine in this model.^{8a} Consistent with the effective *in vivo* inhibition of arginase, treatment with nebulized A1P ($80 \mu\text{g/g}$) attenuated significantly the total resistance of the respiratory system (R) following methacholine challenge in OVA/OVA mice (Figure 6A). Similarly, the maximum resistance of the central airways (R_N) was significantly attenuated by A1P treatment in the same mice (Figure 6B).

Discussion

Imidazole and related azoles are well-known ligands in metalloenzyme active sites, and ongoing explorations of azole derivatives as potential pharmacophores have inspired the current study. For example, spectroscopic studies on the binding of imidazole and its analogues 1,2,3-triazole, 1,2,4-triazole, and tetrazole to Co^{2+} -substituted human carbonic anhydrase I and bovine carbonic anhydrase II suggest that 1,2,3-triazole forms a pentacoordinated metal complex while 1,2,4-triazole and tetrazole bind in tetrahedral metal complexes.³⁷ The crystal structure of human carbonic anhydrase I complexed with imidazole reveals the inhibitor bound via one of its nitrogen atoms as a fifth ligand to the Zn^{2+} ion,³⁸ and the structure of human carbonic anhydrase II complexed with 1,2,4-triazole shows that the heterocycle coordinates to Zn^{2+} through the N4 atom.³⁹ In other systems, the X-ray crystal structure of methionine aminopeptidase-2 in complex with a 1,2,4-triazole derivative reveals a novel binding mode that

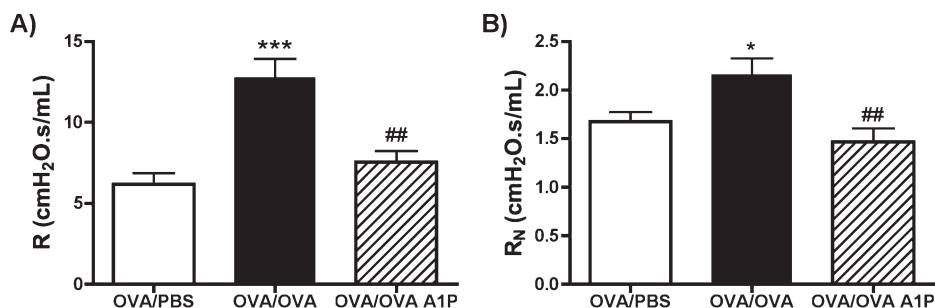


Figure 6. Impact of arginase inhibition by A1P in the acute ovalbumin (OVA)-sensitization and -challenge murine model of allergic airways inflammation. (A) A1P attenuated significantly the maximum total lung resistance (R) evoked by methacholine challenge in mice sensitized to OVA and challenged with nebulized vehicle (OVA/PBS) or OVA (OVA/OVA and OVA/OVA A1P). (B) A1P also notably decreased the maximum methacholine-induced increase in central airways responsiveness (R_N) in the same animal model. Values are expressed as the mean \pm SE ($n = 12$ /group): (*) $P < 0.05$; (***) $P < 0.0001$ to OVA/PBS; (##) $P < 0.01$ to OVA/OVA.

may account for nanomolar affinity: two of the heterocyclic N atoms coordinate the Co^{2+} ion, while the third one makes a hydrogen bond to a histidine residue in the active site.⁴⁰ Finally, a common binding mode for imidazole-based heme oxygenase-1 inhibitors has been recently reported, revealing that the imidazole group coordinates to the heme iron.⁴¹

In contrast with imidazole and the azoles described above, 2-aminoimidazoles have had only limited study in the design of metalloenzymes inhibitors. To our knowledge, the only examples reported to date are those studied as inhibitors of NO synthase.^{28,42} Optical absorption, magnetic circular dichroism, and electronic paramagnetic resonance analyses of endothelial nitric oxide synthase complexed with imidazole derivatives suggest the direct binding of 2-aminoimidazole to the guanidine binding subdomain near the catalytic heme group.⁴² Accordingly, such derivatives are considered promising ligands for exploring the active sites of different forms of nitric oxide synthase and for the development of isozyme-selective inhibitors. Some 2-amino-5-azolylpentanoic acids related to L-ornithine have also been reported as nitric oxide synthase inhibitors.²⁸ However, we have determined that the 2-aminoimidazole amino acids shown in Table 1 are only weak or modest inhibitors of recombinant rat neuronal nitric oxide synthase (nNOS) or recombinant murine inducible nitric oxide synthase (iNOS), with IC_{50} values ranging from 65 to 3300 μM (data not shown). Moreover, the new lead arginase inhibitor identified in the current study, A1P (**10**), is only a weak inhibitor of iNOS and nNOS, with IC_{50} values of 480 and 135 μM , respectively (data not shown). Such selectivity for arginase inhibition may facilitate the use of A1P and its derivatives for the selective modulation of L-arginine levels in the management of diseases associated with aberrant L-arginine homeostasis.

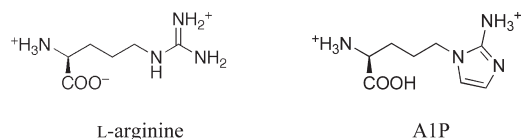
Notably, *in vitro* SARs based on biological assays and X-ray crystallographic studies show a clear correlation of inhibitor potency with the length of the carbon linker separating the heterocycle and the amino acid moieties; the highest efficacy observed for A1P is associated with a side chain that is the same length as that of the natural substrate, L-arginine. Interestingly, 2-aminoimidazoles smaller than L-arginine (2AI and 2AH) are noncompetitive inhibitors, whereas inhibitors that are more isosteric with L-arginine (AHH and A1P) are competitive inhibitors. The orientation of the 2-aminoimidazole moiety as it is attached to the amino acid side chain is a critical affinity determinant, as shown by differences in the inhibitory potencies of A1P, A4P, and APP. Since the pK_a of the 2-aminoimidazole moiety is relatively invariant to

alkylation on imidazole N or C atoms,²² differences in pK_a cannot contribute to differences in inhibitor affinity. Accordingly, the optimal affinity of A1P in the series of compounds shown in Table 1 correlates with a 2-aminoimidazole orientation that is most closely isosteric with the guanidinium moiety of the arginase substrate L-arginine. We speculate that this optimizes enzyme–inhibitor metal coordination interactions.

Human asthma patients have increased levels of expression and activity of arginase I in the airways,⁸ similar to the mouse model of OVA-induced airways inflammation⁴³ used in this study. Recently, we have demonstrated that arginase inhibition by the boronic acid derivative BEC reduces airways hyperresponsiveness in murine models of allergic airways inflammation.^{8a} The current study indicates that A1P is similarly effective *in vivo* as an arginase inhibitor in this acute asthma model.

Summary and Conclusions

This is the first investigation of arginase inhibition using the 2-aminoimidazole moiety as a “warhead” to target the binuclear manganese cluster. Importantly, A1P is a mimetic of the substrate L-arginine in which the side chain N_ϵ and N_γ atoms are covalently linked via the imidazole heterocycle:



Incorporation of the guanidinium nitrogen atoms within the imidazole moiety serves to depress the pK_a of the side chain to ~ 7 – 8 , which can also lead to improved bioavailability. Our SAR analysis demonstrates that the 2-aminoimidazole moiety can target metal coordination and hydrogen bond interactions in the enzyme active site. The most potent inhibitor studied, A1P, exhibits low micromolar binding affinity. Moreover, A1P inhibits arginase *in vivo* and significantly reduces airways hyperresponsiveness to methacholine in OVA-sensitized and -challenged Balb/C mice. Only three other types of amino acid inhibitors are known to bind to arginase with low micromolar affinity or better: those bearing boronic acid side chains,^{13b,18} one bearing an *N*-hydroxyguanidinium side chain,⁴⁴ and one bearing an *N*-hydroxyamino side chain (*N*-hydroxy-L-lysine).⁴⁵ Therefore, we now add the 2-aminoimidazole amino acid A1P to this important group of lead compounds for the development of

new arginase inhibitors that may exhibit alternative and improved pharmacokinetic profiles.

Experimental Section

Synthesis of 2-Aminoimidazole Amino Acids. General Procedures. All reagents were of at least 95% purity, purchased from Sigma Aldrich Co., Fisher Scientific, or Alfa Aesar and used as received. All solvents were of HPLC grade and purchased from Fisher Scientific or Sigma Aldrich Co. For anhydrous conditions, solvents were freshly distilled under N₂ (Et₂O from Na, CH₂Cl₂ from P₂O₅, and THF from Na/benzophenone). Reactions were monitored by TLC with Sigma-Aldrich aluminum plates (silica gel F₂₅₄, 60 Å, 0.25 mm), visualized by quenching under UV light, equilibrating in a glass chamber containing iodine, and/or staining with ninhydrin solution. Flash column chromatography was performed using Fisher Scientific silica gel 60 (230–400 mesh). HPLC was performed on a Waters system with a 1525 binary pump and a 2487 dual λ absorbance UV detector (detection at 254 nm), using a Symmetry (C18) 5 μM column (4.6 mm × 150 mm) (MeCN/H₂O/TFA, 10:90:0.1; isocratic elution). Mass spectrometry was carried out on Waters Acquity SQD UPLC-MS (low resolution) and on LCT Premier XE Micromass/Waters MS Technologies (high resolution) spectrometers. Purities of all synthesized and tested compounds were greater than 95%.

¹H and ¹³C NMR spectra were recorded on Bruker DMX 360 and DRX 500 spectrometers at 360 and 500 MHz, respectively, for ¹H and at 90.6 and 125.6 MHz, respectively, for ¹³C NMR. Assignments were made on the basis of chemical shifts, signal intensity, COSY, and HMQC sequences. ¹H and ¹³C NMR chemical shifts (δ) are reported in ppm relative to the residual solvent peaks. ¹H NMR coupling constants (*J*) are reported in Hz, and multiplicities are denoted as follows: s, singlet; d, doublet; t, triplet; m, multiplet; bs, broad singlet.

2-Bis(*tert*-butyloxycarbonyl)amino-1-*tert*-butyloxycarbonylimidazole (5). 2-Aminoimidazolium sulfate (5.5 g, 41.5 mmol) was dissolved in water (25 mL) and treated with a solution of NaOH (1.7 g, 42.5 mmol) in water (3 mL). The water was removed under reduced pressure. The residue was extracted with MeOH (30 mL), and the methanolic extracts were rotoevaporated to dryness. The resulting light-brown oil was suspended in MeCN (30 mL). Then NEt₃ (20 mL) and DMAP (1 g) were added. The suspension was cooled to 0 °C. Then di-*tert*-butyl pyrocarbonate (27.6 g, 166 mmol) in MeCN (30 mL) was added dropwise. The mixture was stirred at 20 °C for 16 h, after which di-*tert*-butyl pyrocarbonate (6.9 g, 41.5 mmol) in MeCN (15 mL) was added. The resulting suspension was refluxed for 8 h. The solvent was rotoevaporated and the residue partitioned between CH₂Cl₂ (200 mL) and water (100 mL). The aqueous layer was reextracted with CH₂Cl₂ (4 × 50 mL), and the combined organic extracts were washed with water (100 mL), saturated aqueous NaHCO₃ (100 mL), brine (100 mL), dried (Na₂SO₄), filtered, and concentrated under reduced pressure. Purification by flash column chromatography on SiO₂ (hexane/EtOAc gradients) afforded pure product **5** (10.1 g, 63%) as a colorless oil. ¹H NMR (CDCl₃): δ 7.39 (d, *J* = 1.9, 1H, *HC*-4 of imidazole), 6.93 (d, *J* = 1.9, 1H, *HC*-5 of imidazole), 1.58 (s, 9H, N-1Boc), 1.43 (s, 18H, 2-NBoc₂). ¹³C NMR (CDCl₃): δ 149.4 (2CO, 2-NBoc₂), 146.4 (CO, N1-Boc), 138.3 (C-2 of imidazole), 126.7 (C-4/C-5 of imidazole), 118.5 (C-5/C-4 of imidazole), 86.1 (CMe₃, N-1Boc), 83.6 (2CMe₃, 2-NBoc₂), 27.9 (9CH₃, 3Boc). MS ES+ *m/z* 384.2 (M + H)⁺.

2-Bis(*tert*-butyloxycarbonyl)aminoimidazole (6). To a solution of **5** (1.48 g, 3.9 mmol) in MeOH (20 mL) at room temperature, NH₃ in MeOH (3 mL, 7N) was added. The mixture was stirred at room temperature for 48 h. Then the solvent was removed in vacuo. Purification by flash column chromatography on SiO₂ (hexane/EtOAc gradient) yielded **6** (0.83 g, 56%) as a white solid. ¹H NMR (DMSO-*d*₆): δ 12.13 (s, 1H, *NH* of imidazole), 7.07 (s, 1H, *HC*-4/C-5 of imidazole), 6.80 (s, 1H,

HC-5/C-4 of imidazole), 1.38 (s, 18H, 2Boc). ¹³C NMR (DMSO-*d*₆): δ 156.2 (2CO, 2Boc), 140.7 (C-2 of imidazole), 126.5 (C-4/C-5 of imidazole), 116.3 (C-5/C-4 of imidazole), 82.6 (2CMe₃, 2Boc), 27.4 (6CH₃, 2Boc). MS ES+ *m/z* 284.2 (M + H)⁺.

2-[Bis(*tert*-butyloxycarbonyl)amino]-5-[2-bis(*tert*-butyloxycarbonyl)aminoimidazol-1-yl]pentanoic Acid *tert*-Butyl Ester (9). Anhydrous K₂CO₃ (0.77 g, 5.6 mmol) was suspended in DMF (7.5 mL) and purged with N₂ for 5 min. **6** (0.80 g, 2.8 mmol) was added in one portion under N₂ purging, followed by the bromide **8** (1.3 g, 2.9 mmol) in DMF (3 mL). The mixture was warmed to 60 °C while stirring vigorously and purging with N₂. Then the N₂ line was removed and stirring was continued overnight at 60 °C under inert atmosphere. The reaction mixture was allowed to cool at room temperature, poured into cold water (50 mL), and extracted with CH₂Cl₂ (5 × 40 mL). The combined organic extracts were washed with water (50 mL), brine (50 mL), dried (Na₂SO₄), filtered, and concentrated. Flash chromatography on silica gel (hexane/EtOAc gradients) afforded **9** (1.1 g, 60%) as a light-brown oil. ¹H NMR (CDCl₃): δ 7.00 (d, *J* = 1.2, 1H, *HC*-4/C-5 of imidazole), 6.89 (d, *J* = 1.2, 1H, *HC*-5/C-4 of imidazole), 4.69 (dd, *J* = 8.4, 5.6, 1H, *CH*COO), 3.73 (dd, *J* = 7.1, 5.8, 2H, *CH*₂N), 2.1–1.81 (m, 4H, *CH*CH₂ + *CH*CH₂CH₂), 1.48 (s, 18H, 2Boc), 1.42 (s, 18H, 2Boc), 1.41 (s, 9H, 3CH₃ of COO^tBu). ¹³C NMR (CDCl₃): δ 169.5 (CO, COO^tBu), 152.9 (3CO, 3Boc), 150.1 (CO, Boc), 138.2 (C-2 of imidazole), 127.2 (C-4/C-5 of imidazole), 118.7 (C-5/C-4 of imidazole), 83.4 (2CMe₃, 2Boc), 81.9 (2CMe₃, 2Boc), 77.6 (CMe₃, COO^tBu), 58.5 (CHCOO), 45.3 (CH₂N), 28.4 (6CH₃, 2Boc), 28.2 (6CH₃, 2Boc), 28.1 (3CH₃ of COO^tBu), 27.2 (CHCH₂), 26.9 (CHCH₂CH₂). MS ES+ *m/z* 655.4 (M + H)⁺.

2-(*S*)-Amino-5-(2-aminoimidazol-1-yl)pentanoic Acid Ammonium Salt (A1P, 10). The Boc-protected derivative **9** (0.65 g, 1 mmol) was dissolved in CH₂Cl₂ (4 mL), cooled at 0 °C (water/ice bath), and treated dropwise with TFA (4 mL) with constant stirring. The flask was allowed to reach room temperature and the mixture stirred for another 4 h until TLC monitoring (MeOH/CH₂Cl₂, 5:95) revealed complete deprotection. Evaporation, washing with CHCl₃, and drying under vacuum yielded **10** (0.39 g, 92%) as a bis-trifluoroacetate salt. Further purification by flash column chromatography (CHCl₃/MeOH/NH₃ gradients) afforded **10** (0.31 g) as a colorless oil. ¹H NMR (D₂O): δ 6.80 (s, 1H, *HC*-4 of imidazole), 6.70 (s, 1H, *HC*-5 of imidazole), 3.86 (m, 2H, *CH*₂N), 3.66 (m, 1H, *CH*COO), 1.83 (m, 4H, 2CH₂). ¹³C NMR (D₂O): δ 176.2 (CO), 147.5 (C-2 of imidazole), 119.1 (C-4 of imidazole), 116.4 (C-5 of imidazole), 54.5 (CHCOO), 44.1 (CH₂N), 28.2 (CHCH₂CH₂CH₂N), 24.6 (CHCH₂CH₂CH₂N). A1P⁻Na⁺ (pH 14): ¹H NMR (D₂O + NaOD): δ 6.61 (s, 1H, *HC*-4 of imidazole), 6.46 (s, 1H, *HC*-5 of imidazole), 3.63 (m, 2H, *CH*₂N), 3.11 (m, 1H, *CH*COO), 1.60 (m, 2H, CHCH₂CH₂CH₂N), 1.44 (m, 2H, CHCH₂CH₂CH₂N). A1P · 2HCl (pH 1): ¹H NMR (D₂O): δ 6.75 (bs, 2H, *HC*-4, *HC*-5 of imidazole), 3.96 (t, *J* = 5.8, 1H, *CH*COO), 3.84 (t, *J* = 6.4, 2H, *CH*₂N), 1.84 (m, 4H). HRMS *m/z* 199.1188 (calcd for M + H, 199.1195).

2-[Bis(*tert*-butyloxycarbonyl)amino]-5-(imidazol-2-ylamino)-pentanoic Acid *tert*-Butyl Ester (11). 2-Aminoimidazolium sulfate (**2** g, 15 mmol) was dissolved in water (10 mL) and treated with NaOH (0.6 g, 15 mmol) in water (3 mL). The solvent was removed under vacuum and the evaporation residue washed with EtOH (50 mL), then sonicated in EtOH (50 mL) for 10 min to ensure the complete extraction of **11** from the inorganic salt matrix. The resulting light-brown solution was filtered and the inorganic precipitate washed with EtOH (3 × 10 mL). Rotoevaporation to dryness of the combined EtOH extracts yielded the 2-aminoimidazole free base (1.25 g, 99%) as a brown oil. The crude product was retaken in MeOH (10 mL), aldehyde **4** (3 g, 7.75 mmol) was added, and the resulting mixture was treated with NaBH₃CN (300 mg, 4.7 mmol) and activated molecular sieves (4 Å, 2 g). The suspension was stirred at room temperature until TLC indicated no further advancement of the reaction

(48 h). Column chromatography of the residue (silica gel, hexane/EtOAc gradient) yielded **11** (1.05 g, 30%) as a purple oil (the alcohol **7** was the major byproduct and could be recovered: 1.8 g, 60% conversion). $^1\text{H NMR}$ (CDCl_3): δ 10.03 (s, 1H, NH of imidazole), 6.55 (s, 1H, HC-4/C-5 of imidazole), 6.49 (s, 1H, HC-5/C-4 of imidazole), 5.22 (t, $J=6.1$, 1H, NH-2 of imidazole), 4.64 (dd, $J=9.8, 4.8$, 1H, CHCOO), 3.30 (dd, $J=7.0, 6.5$, 2H, CH_2N), 2.10–1.67 (m, 4H, $\text{CHCH}_2 + \text{CHCH}_2\text{CH}_2$), 1.50 (s, 18H, 2Boc), 1.43 (s, 9H, 3CH_3 of COO^tBu). $^{13}\text{C NMR}$ (CDCl_3): δ 169.8 (CO, COO^tBu), 153.4 (2CO, 2Boc), 148.1 (C-2 of imidazole), 121.8 (C-4 of imidazole), 111.0 (C-5 of imidazole), 84.0 (2CMe₃, 2Boc), 82.1 (CMe₃, COO^tBu), 58.7 (CHCOO), 43.3 (CH_2N), 28.3 (6CH₃, 2Boc), 28.2 (3CH₃ of COO^tBu), 26.6 (CHCH_2), 25.8 (CHCH_2CH_2). HRMS m/z 455.2856 (calcd for M + H, 455.2870).

(S)-2-Amino-5-(imidazol-2-ylamino)pentanoic Acid (APP) (12). The same general procedure as for the synthesis of **10** afforded **12** as a bis-trifluoroacetate salt (90%). $^1\text{H NMR}$ (D_2O): δ 6.87 (bs, 2H, HC-4, HC-5 of imidazole), 4.01 (m, 1H, CHCOO), 3.32 (m, 2H, CH_2N), 2.05 (m, 2H, CHCH_2), 1.80 (m, 2H, CHCH_2CH_2). $^{13}\text{C NMR}$ (D_2O): δ 165.5 (CO), 146.7 (C-2 of imidazole), 113.4 (C-4 of imidazole), 112.9 (C-5 of imidazole), 60.6 (CHCOO), 42.5 (CH_2N), 29.5 ($\text{CHCH}_2\text{CH}_2\text{CH}_2\text{N}$), 26.5 ($\text{CHCH}_2\text{CH}_2\text{CH}_2\text{N}$) (signals from TFA were omitted).

Dimethyl 2,6-Bis(tert-butoxycarbonylamino)heptanedioate (13). 2,6-Diaminopimelic acid (6 g, 31.5 mmol) was dissolved in MeOH (50 mL) under N_2 purging in an oven-dried flask. The suspension was cooled to -5 to -10 °C (ice/acetone bath) and treated dropwise with thionyl chloride (5.1 mL, 69.4 mmol). The mixture was stirred at -5 to -10 °C for 1 h, then overnight at room temperature, when $^1\text{H NMR}$ and TLC monitoring ($\text{CHCl}_3/\text{MeOH}/\text{NH}_4\text{OH}$, 2:8:1) indicated completion of the reaction. The solvent was rotoevaporated and the crude product washed with Et_2O , then dried overnight under vacuum to yield the corresponding amino ester (8.5 g) as a dihydrochloride salt. NEt_3 (12.3 mL) and DMAP (2.9 g) were added to a suspension of the amino ester in MeCN (80 mL). The suspension was cooled to 0 °C. Then di-*tert*-butyl pyrocarbonate (25.8 g, 118.1 mmol) in MeCN (30 mL) was added dropwise. The mixture was stirred at room temperature for 48 h. Solvent rotoevaporation and purification by flash column chromatography (silica gel, hexane/EtOAc gradients) afforded **13** as a light-yellow oil (88%). $^1\text{H NMR}$ (CDCl_3): δ 5.09 (m, 2H, 2CHCOO), 4.26 (m, 2H, 2NH), 3.72 (s, 6H, 2COOCH₃), 1.82 (m, 2H, C_AH₂CH), 1.63 (m, 2H, C_BH₂CH), 1.43 (s, 18H, 2Boc), 1.39 (m, 2H, CH₂CH₂CH). $^{13}\text{C NMR}$ (CDCl_3): δ 173.5 (2CO, 2COOMe), 155.8 (2CO, 2Boc), 80.34 (2CMe₃, 2Boc), 53.5 (C_AH), 52.7 (C_BH), 32.7 (C_AH₂CH), 32.6 (C_BH₂CH), 28.6 (6CH₃, 2Boc), 21.8 (C_AH₂CH₂CH), 21.6 (C_BH₂CH₂CH). MS ES+ m/z 419.2 (M + H)⁺.

Methyl 2,6-Bis(tert-butoxycarbonylamino)-7-oxoheptanoate (14). **13** (1.2 g, 2.86 mmol) was dissolved in Et_2O (30 mL) with stirring at room temperature and nitrogen purging, then cooled to -78 °C (acetone/dry ice bath). DIBAH (1 M) in hexane (1.86 mL, 1.86 mmol) was added dropwise. $^1\text{H NMR}$ monitoring indicated completion of the reaction after 1 h. The reaction mixture was quenched with water (5 mL) and filtered. The filtrate was rotoevaporated to dryness, washed with CHCl_3 , and dried overnight under vacuum to afford **14** (0.99 g, 89%) as a colorless oil. $^1\text{H NMR}$ (CDCl_3): δ 9.57 (s, 1H, CHO), 5.09 (m, 2H, CHCHO + CHCOOMe), 4.27 (m, 2H, 2NH), 3.73 (s, 3H, COOCH₃), 1.80 (m, 2H, C_AH₂CH), 1.64 (m, 2H, C_BH₂CH), 1.44 (s, 18H, 2Boc), 1.40 (m, 2H, CH₂CH₂CH). $^{13}\text{C NMR}$ (CDCl_3): δ 200.0 (CHO), 173.4 (CO, COOMe), 155.9 (2CO, 2Boc), 80.3 (2CMe₃, 2Boc), 59.8 (CHCHO), 53.4 (C_AH), 52.6 (C_BH), 32.8 (C_AH₂CH), 32.6 (C_BH₂CH), 28.6 (6CH₃, 2Boc), 21.7 (C_AH₂CH₂CH), 21.5 (C_BH₂CH₂CH), 21.3 (C_CH₂CH₂CH). MS ES+ m/z 389.2 (M + H)⁺.

2-Amino-5-(2-aminoimidazol-4-yl)pentanoic Acid (A4P, 16) (1.6 g, 4.12 mmol) was stirred in EtOAc (32 mL) and 4 N HCl (30 mL) at room temperature for 2 h. The solvent was rotoevaporated,

and the resulting light-brown oil was dried overnight under vacuum, then resolubilized in water (18 mL). The pH was adjusted to 4.5 with 2 N NaOH, and cyanamide (1.04 g) was added in one portion. The reaction mixture was refluxed at 95 °C for 3 h, then rotoevaporated to dryness. Purification by flash column chromatography ($\text{CHCl}_3/\text{MeOH}/\text{NH}_4\text{OH}$ gradients) generated **16** (0.23 g, 30%) as a light-yellow oil. $^1\text{H NMR}$ (D_2O): δ 6.77 (s, 1H, HC-4 of imidazole), 3.75 (m, 1H, CHCOO), 2.55 (m, 2H, $\text{CHCH}_2\text{CH}_2\text{CH}_2$ -imidazole), 1.88 (m, 2H, $\text{CHCH}_2\text{CH}_2\text{CH}_2$ -imidazole), 1.68 (m, 2H, $\text{CHCH}_2\text{CH}_2\text{CH}_2$ -imidazole). $^{13}\text{C NMR}$ (D_2O): δ 175.1 (CO), 147.1 (C-2 of imidazole), 128.4 (C-4 of imidazole), 109.4 (C-5 of imidazole), 54.6 (CHCOO), 29.9 ($\text{CHCH}_2\text{CH}_2\text{CH}_2$ -imidazole), 23.9 ($\text{CHCH}_2\text{CH}_2\text{CH}_2$ -imidazole), 23.3 ($\text{CHCH}_2\text{CH}_2\text{CH}_2$ -imidazole). HRMS m/z 199.1189 (calcd for M + H, 199.1195).

Kinetic Assays. 2-Aminoimidazole amino acids affinities for human arginase I were determined using the fixed point assay with [^{14}C -guanidino]-L-arginine³⁴ as previously reported.⁴⁶ Recombinant human arginase I was prepared as previously described.¹⁹ The final working concentrations in the reaction tubes were 1 mM for the unlabeled L-arginine and 0.07 $\mu\text{g}/\mu\text{L}$ for human arginase I. Data analysis was based on the kinetic replot v_0/v_i as a function of inhibitor concentration, where v_0 and v_i were the observed velocities in the absence and presence of inhibitor, respectively. The mode of inhibition (i.e., noncompetitive or competitive) was determined from Lineweaver–Burk plots of kinetic data at several different inhibitor concentrations.

Surface Plasmon Resonance. The binding affinity of AIP was determined on a Biacore 3000 instrument, following a previously reported procedure,³² except that all measurements were made at pH 8.5 and the analyte concentrations ranged from 0 to 800 μM . Binding data were analyzed using a 1:1 Langmuir interaction model.⁴⁷

Crystallography. Crystals of human arginase I complexed with 2AH were prepared by soaking 2AH into preformed crystals of the native enzyme, which were prepared by the hanging drop vapor diffusion method at 21 °C. Drops containing 3 μL of protein solution [3.5 mg/mL protein, 50.0 mM bicine (pH 8.5), 2 mM thymine, 100 μM MnCl_2] and 3 μL of precipitant solution [0.1 M HEPES (pH 7.0), 28% Jeffamine] were equilibrated against a 1 mL reservoir of precipitant buffer. Crystals generally formed within 3–4 days. Crystals were harvested and soaked in a precipitant solution augmented with 20 mM 2AH for 1 week and then cryoprotected in a precipitant solution containing 32% Jeffamine prior to flash cooling in liquid nitrogen.

Crystals of the human arginase I–AHH and human arginase I–2 aminoimidazole complexes were prepared by cocrystallization in hanging drops at 21 °C. Drops containing 3 μL of protein solution [3.5 mg/mL protein, 50 mM bicine (pH 8.5), 2 mM AHH or 2 mM 2-aminoimidazole, 100 μM MnCl_2] and 3 μL of precipitant solution [0.1 M HEPES (pH 7.0), 28% Jeffamine] were equilibrated against a 1 mL reservoir of precipitant solution. Crystals appeared overnight and grew with typical dimensions of 0.5 mm \times 0.2 mm \times 0.2 mm within 1 week. Crystals were soaked for 24 h in a precipitant solution augmented with 5 mM AHH or 2-aminoimidazole and cryoprotected as described above.

X-ray diffraction data from all crystals were collected at the National Synchrotron Light Source beamline X6A. Diffraction intensities measured from human arginase I–inhibitor complexes exhibited symmetry consistent with apparent space group *P*6 (unit cell parameters $a=b=90.1$ Å, $c=69.7$ Å). Intensity data integration and reduction were performed using the HKL2000 suite of programs.⁴⁸ Data reduction statistics are recorded in Table 2. As with crystals of other human arginase I complexes,⁴⁹ deviations from ideal Wilson statistics were observed with $\langle I^2 \rangle / \langle I \rangle^2 = 1.5$, indicating perfect hemihedral twinning.⁵⁰ The structure of each enzyme–inhibitor complex was solved by molecular replacement using the program Phaser⁵¹ with chain A of the

Table 2. Data Collection and Refinement Statistics

	human arginase I–2AI	human arginase I–2AH	human arginase I–AHH
Data Collection			
resolution, Å	50.0–1.90	50.0–1.47	50.0–1.90
total/unique reflections measured	91110/50007	196796/107754	95366/50344
$R_{\text{merge}}^{a,b}$	0.061 (0.265)	0.059 (0.616)	0.086 (0.310)
$I/\sigma(I)^a$	13.9 (4.0)	21.1 (2.3)	15.4 (3.8)
completeness, % ^a	99.1 (98.7)	99.4 (99.6)	99.8 (100.0)
Refinement			
reflections used in refinement/test set	47507/2500	102365/5389	49288/2184
R_{twin}^c	0.168	0.149	0.141
$R_{\text{twin/free}}^c$	0.176	0.162	0.190
Protein atoms ^d	4772	4772	4762
water molecules ^d	246	460	338
inhibitor atoms ^d	12	24	26
manganese ions ^d	4	4	4
sulfate ions ^d		2	
Root-Mean-Square Deviation			
bond length, Å	0.007	0.011	0.008
bond angle, deg	2.1	2.2	2.1
PDB accession code	3MJL	3MFW	3MFV

^aNumber in parentheses refer to the outer 0.1 Å shell of data. ^b $R_{\text{merge}} = \sum |I - \langle I \rangle| / \sum I$, where I is the observed intensity and $\langle I \rangle$ is the average intensity calculated for replicate data. ^c $R_{\text{twin}} = \sum [|F_{\text{calc}/A}|^2 + |F_{\text{calc}/B}|^2]^{1/2} - |F_{\text{obs}}| / \sum |F_{\text{obs}}|$ for reflections contained in the working set. $|F_{\text{calc}/A}|$ and $|F_{\text{calc}/B}|$ are the structure factor amplitudes calculated for the separate twin domains A and B, respectively. R_{twin} underestimates the residual error in the model over the two twin-related reflections by a factor of approximately 0.7. The same expression describes $R_{\text{twin/free}}$, which was calculated for test set reflections excluded from refinement. ^dPer asymmetric unit.

unliganded human arginase I (PDB accession code 2ZAV, less water molecules)⁴⁹ used as a search probe against twinned data. In order to calculate electron density maps, structure factor amplitudes ($|F_{\text{obs}}|$) derived from twinned intensity data ($|I_{\text{obs}}|$) were deconvoluted into structure factor amplitudes corresponding to individual twin domains A and B ($|F_{\text{obs}/A}|$ and $|F_{\text{obs}/B}|$, respectively) using the structure-based algorithm of Redinbo and Yeates⁵⁰ implemented in CNS.⁵²

Crystallographic refinement of each enzyme–inhibitor complex against twinned data was performed as previously described using CNS.⁴⁹ In the later stages of each refinement, after the majority of water molecules were located, gradient omit maps revealed the inhibitor bound in the active site of each monomer in the asymmetric unit.

Inhibitors were refined with full occupancy and atomic B factors consistent with the average B -factor calculated for the entire protein. For the refinement of the human arginase I–2-aminoimidazole and human arginase I–2AH complexes, full-matrix least-squares refinement was performed against twinned data using the program Shelx⁵³ in the final stages of refinement. Isotropic B factors were used in refinement with the exception of the manganese ions and sulfur atoms in the human arginase I–2AH complex, which were refined anisotropically (Table 2).

Disordered segments were excluded from the final models of the human arginase I–AHH complex (M1-S5 and N319-K322), the human arginase I–2-aminoimidazole complex (M1-S5 and N319-K322), and the human arginase I–2AH complex (M1-K4 and N319-K322). The quality of each refined model was assessed using PROCHECK.⁵⁴

Acute Murine OVA-Sensitization and Challenge Model of Allergic Airways Inflammation. These protocols were approved by the University of Toronto Faculty Advisory Committee on Animal Services and were conducted in accordance with the

guidelines of the Canadian Council on Animal Care. The acute model utilized a 3-week OVA-sensitization and -challenge protocol, as described previously.^{8a} Briefly, female Balb/C mice (6–8 weeks old, Charles River Laboratories, Saint-Constant, PQ) were sensitized to chicken OVA on days 0 and 7 (ip, 25 μg of chicken OVA; grade V, >98% pure; Sigma Chemical Company, Mississauga, Ontario, Canada), with 1 mg of aluminum hydroxide gel (Invitrogen, Grand Island, NY). Beginning on day 14, animals were randomized to repeated exposure to nebulized 6% OVA in PBS or PBS alone for 25 min/day on days 14–20, using an AeroNebLab nebulizer (SciReq Inc., Montréal PQ).

In Vivo Arginase Inhibition with A1P and Methacholine Challenge. On day 21, 24 h after the final OVA or PBS challenge, mice were anesthetized with 50 mg/kg ketamine (Bioniche, Belleville, Ontario, Canada) and 10 mg/kg xylazine (Bayer Inc., Toronto, Ontario, Canada) prior to intubation with an 18G stainless steel cannula (BD Biosciences Canada, Mississauga, Ontario, Canada) for in vivo, ventilator-based assessment of methacholine-responsiveness using the FlexiVent system Scireq. After determination of baseline pulmonary resistance parameters, A1P (80 μg/g body weight) was delivered via nebulization directly into the ventilatory circuit of a randomly selected subgroup of OVA/OVA mice. In a previous study we showed that arginase inhibition did not exhibit any effect on OVA/PBS mice. Fifteen minutes after delivery of the drug, baseline pulmonary resistance was reassessed and the methacholine dose–response curve was initiated, as previously described.^{8a} In brief, mice were challenged with methacholine (0–100 mg/mL in sterile PBS; Sigma) nebulized directly into the ventilatory circuit (AeroNebLab nebulizer). All data points were collected using the FlexiVent software (Scireq Inc.) and analyzed off-line using Excel (Microsoft Corp., Redmond, WA). We have previously shown^{8a} that this treatment-based protocol completely abrogates the allergic airways-induced hyperresponsiveness to methacholine in several murine models of allergic airways inflammation.

Acknowledgment. This work was supported by the America Asthma Foundation and NIH Grant GM49758. We thank Dr. Steven Seeholzer, Dr. Hua Ding, and the Protein Core Facility at Children's Hospital of Philadelphia, PA, for assistance with surface plasmon resonance measurements, and Dr. Rakesh Kohli for recording the HRMS spectra of the compounds. We also thank the National Synchrotron Light Source, beam time X6A, for access to X-ray crystallographic data collection facilities. D.W.C. is a Senior Fellow of the American Asthma Foundation. M.L.N. is a recipient of CIHR and Ontario Thoracic Society Doctoral Awards. J.A.S. is a Scientist in the Keenan Research Centre in the Li Ka Shing Knowledge Institute of St. Michael's Hospital.

References

- (1) (a) Borcic, O.; Straus, B. Separation of arginase isoenzymes from human tissues by agar gel electrophoresis. *J. Clin. Chem. Clin. Biochem.* **1976**, *14*, 533–535. (b) Grody, W. W.; Dizikes, G. J.; Cederbaum, S. D. Human arginase isozymes. *Isozymes: Curr. Top. Biol. Med. Res.* **1987**, *13*, 181–214. (c) Jenkinson, C. P.; Grody, W. W.; Cederbaum, S. D. Comparative properties of arginases. *Comp. Biochem. Physiol.* **1996**, *114B*, 107–132. (d) Ash, D. E.; Cox, J. D.; Christianson, D. W. Manganese and Its Role in Biological Processes. In *Metal Ions in Biological Systems*; Sigel, A., Sigel, H., Eds.; M. Dekker: New York, 2000; Vol. 37, pp 407–428.
- (2) Morris, S. M., Jr. Regulation of enzymes of the urea cycle and arginine metabolism. *Annu. Rev. Nutr.* **2002**, *22*, 87–105.
- (3) (a) Morris, S. M., Jr.; Bhamidipati, D.; Kepka-Lenhart, D. Human type II arginase: sequence analysis and tissue-specific expression. *Gene* **1997**, *193*, 157–161. (b) Gotoh, T.; Araki, M.; Mori, M. Chromosomal localization of the human arginase II gene and tissue distribution of its mRNA. *Biochem. Biophys. Res. Commun.* **1997**, *233*, 487–491.
- (4) (a) Christianson, D. W. Arginase: structure, mechanism, and physiological role in male and female sexual arousal. *Acc. Chem.*

- Res.* **2005**, *38*, 191–201. (b) Dowling, D. P.; Di Costanzo, L.; Gennadios, H. A.; Christianson, D. W. Evolution of the arginase fold and functional diversity. *Cell. Mol. Life Sci.* **2008**, *65*, 2039–2055.
- (5) (a) Wu, G.; Morris, S. M., Jr. Arginine metabolism: nitric oxide and beyond. *Biochem. J.* **1998**, *336*, 1–17. (b) Morris, S. M., Jr. Arginine metabolism: boundaries of our knowledge. *J. Nutr.* **2007**, *137*, 1602S–1609S. (c) Morris, S. M., Jr. Recent advances in arginine metabolism: roles and regulation of the arginases. *Br. J. Pharmacol.* **2009**, *157*, 922–930.
- (6) (a) Smith, R. J.; Phang, J. M. The importance of ornithine as a precursor for proline in mammalian cells. *J. Cell. Physiol.* **1979**, *98*, 475–482. (b) Albina, J. E.; Abate, J. A.; Mastrofrancesco, B. Role of ornithine as a proline precursor in healing wounds. *J. Surg. Res.* **1993**, *55*, 97–102. (c) Nieves, C., Jr.; Langkamp-Henken, B. Arginine and immunity: a unique perspective. *Biomed. Pharmacother.* **2002**, *56*, 471–482.
- (7) (a) Kim, P. S.; Iyer, R. K.; Lu, K. V.; Yu, H.; Karimi, A.; Kern, R. M.; Tai, D. K.; Cederbaum, S. D.; Grody, W. W. Expression of the liver form of arginase in erythrocytes. *Mol. Gen. Metab.* **2002**, *76*, 100–110. (b) Wei, L. H.; Wu, G.; Morris, S. M., Jr.; Ignarro, L. J. Elevated arginase I expression in rat aortic smooth muscle cells increases cell proliferation. *Proc. Natl. Acad. Sci. U.S.A.* **2001**, *98*, 9260–9264.
- (8) (a) North, M. L.; Khanna, N.; Marsden, P. A.; Grasmann, H.; Scott, J. A. Functionally important role for arginase I in the airway hyperresponsiveness of asthma. *Am. J. Physiol.: Lung Cell. Mol. Physiol.* **2009**, *296*, L911–L920. (b) Bergeron, C.; Boulet, L.-P.; Page, N.; Laviolette, M.; Zimmermann, N.; Rothenberg, M. E.; Hamid, Q. Influence of cigarette smoke on the arginine pathway in asthmatic airways: increased expression of arginase I. *J. Allergy Clin. Immunol.* **2007**, *119*, 391–397. (c) Zimmermann, N.; King, N. E.; Laporte, J.; Yang, M.; Mishra, A.; Pope, S. M.; Muntel, E. E.; Witte, D. P.; Pegg, A. A.; Foster, P. S.; Hamid, Q.; Rothenberg, M. E. Dissection of experimental asthma with DNA microarray analysis identifies arginase in asthma pathogenesis. *J. Clin. Invest.* **2003**, *111*, 1863–1874.
- (9) (a) Pauleau, A.-L.; Rutschman, R.; Lang, R.; Pernis, A.; Watowich, S. S.; Murray, P. J. Enhancer-mediated control of macrophage-specific arginase I expression. *J. Immunol.* **2004**, *172*, 7565–7573. (b) Zimmermann, N.; Mishra, A.; King, N. E.; Fulkerson, P. C.; Doepker, M. P.; Nikolaidis, N. M.; Kindinger, L. E.; Moulton, E. A.; Aronow, B. J.; Rothenberg, M. E. Transcript signatures in experimental asthma: identification of STAT6-dependent and -independent pathways. *J. Immunol.* **2004**, *172*, 1815–1824.
- (10) (a) Li, H.; Romieu, I.; Sienna-Monge, J.-J.; Ramirez-Aguilar, M.; Estela del Rio-Navarro, B.; Kistner, E. O.; Gjessing, H. K.; Lara-Sanchez, I. C.; Chiu, G. Y.; London, S. J. Genetic polymorphisms in arginase I and II and childhood asthma and atopy. *J. Allergy Clin. Immunol.* **2006**, *117*, 119–126. (b) Litonjua, A. A.; Lasky-Su1, J.; Scheiner, K.; Tantisira, K. G.; Lazarus, R.; Klanderman, B.; Lima, J. J.; Irvin, C. G.; Peters, S. P.; Hanrahan, J. P.; Liggett, S. B.; Hawkins, G. A.; Meyers, D. A.; Bleecker, E. R.; Lange, C.; Weiss, S. T. ARG1 is a novel bronchodilator response gene. Screening and replication in four asthma cohorts. *Am. J. Respir. Crit. Care Med.* **2008**, *178*, 688–694.
- (11) (a) Yang, M.; Rangasamy, D.; Matthei, K. I.; Frew, A. J.; Zimmermann, N.; Mahalingam, S.; Webb, D. C.; Tremethick, D. J.; Thompson, P. J.; Hogan, S. P.; Rothenberg, M. E.; Cowden, W. B.; Foster, P. S. Inhibition of arginase I activity by RNA interference attenuates IL-13-induced airways hyperresponsiveness. *J. Immunol.* **2006**, *177*, 5595–5603. (b) Maarsingh, H.; Zuidhof, A. B.; Bos, I. S. T.; van Duin, M.; Boucher, J.-L.; Zaagsma, J.; Meurs, H. Arginase inhibition protects against allergen-induced airway obstruction, hyperresponsiveness, and inflammation. *Am. J. Respir. Crit. Care Med.* **2008**, *178*, 565–573.
- (12) (a) Meurs, H.; Maarsingh, H.; Zaagsma, J. Arginase and asthma: novel insights into nitric oxide homeostasis and airway hyperresponsiveness. *Trends Pharmacol. Sci.* **2003**, *24*, 450–455. (b) Zimmermann, N.; Rothenberg, M. E. The arginine-arginase balance in asthma and lung inflammation. *Eur. J. Pharmacol.* **2006**, *533*, 253–262. (c) Munder, M. Arginase: an emerging key player in the mammalian immune system. *Br. J. Pharmacol.* **2009**, *158*, 638–651. (d) Munder, M. Role of arginase in asthma: potential clinical applications. *Expert Rev. Clin. Pharmacol.* **2010**, *3*, 17–23.
- (13) (a) Cox, J. D.; Kim, N. N.; Traish, A. M.; Christianson, D. W. Arginase–boronic acid complex highlights a physiological role in erectile function. *Nat. Struct. Biol.* **1999**, *6*, 1043–1047. (b) Kim, N. N.; Cox, J. D.; Baggio, R. F.; Emig, F. A.; Mistry, S. K.; Harper, S. L.; Speicher, D. W.; Morris, S. M.; Ash, D. E.; Traish, A.; Christianson, D. W. Probing erectile function: S-(2-boronoethyl)-L-cysteine binds to arginase as a transition state analogue and enhances smooth muscle relaxation in human penile corpus cavernosum. *Biochemistry* **2001**, *40*, 2678–2688. (c) Cama, E.; Colletuori, D. M.; Emig, F. A.; Shin, H.; Kim, S. W.; Kim, N. N.; Traish, A.; Ash, D. E.; Christianson, D. W. Human arginase II: crystal structure and physiological role in male and female sexual arousal. *Biochemistry* **2003**, *42*, 8445–8451.
- (14) (a) Bivalacqua, T. J.; Hellstrom, W. J. G.; Kadowitz, P. J.; Champion, H. C. Increased expression of arginase II in human diabetic corpus cavernosum: in diabetic-associated erectile dysfunction. *Biochem. Biophys. Res. Commun.* **2001**, *283*, 923–927. (b) Bivalacqua, T. J.; Burnett, A. L.; Hellstrom, W. J. G.; Champion, H. C. Overexpression of arginase in the aged mouse penis impairs erectile function and decreases eNOS activity: influence of in vivo gene therapy of anti-arginase. *Am. J. Physiol.: Heart Circ. Physiol.* **2007**, *292*, H1340–H1351.
- (15) Grasmann, H.; Schwiertz, R.; Matthesen, S.; Racké, K.; Ratjen, F. Increased arginase activity in cystic fibrosis airways. *Am. J. Respir. Crit. Care Med.* **2005**, *172*, 1523–1528.
- (16) (a) Yang, Z.; Ming, X.-F. Endothelial arginase: a new target in atherosclerosis. *Curr. Hypertens. Rep.* **2006**, *8*, 54–59. (b) Nelin, L. D.; Stenger, M. R.; Mallek, D. T.; Chicoine, L. G. Vascular arginase and hypertension. *Curr. Hypertens. Rev.* **2007**, *3*, 242–249. (c) Santhanam, L.; Lim, H. K.; Lim, H. K.; Miriel, V.; Brown, T.; Patel, M.; Balanson, S.; Ryoo, S.; Anderson, M.; Irani, K.; Khanday, F.; Di Costanzo, L.; Nyhan, D.; Hare, J. M.; Christianson, D. W.; Rivers, R.; Shoukas, A.; Berkowitz, D. E. Inducible NO synthase-dependent S-nitrosylation and activation of arginase I contribute to age-related endothelial dysfunction. *Circ. Res.* **2007**, *101*, 692–702. (d) Santhanam, L.; Christianson, D. W.; Nyhan, D.; Berkowitz, D. E. Arginase and vascular aging. *J. Appl. Physiol.* **2008**, *105*, 1632–1642. (e) Ryoo, S.; Gupta, G.; Benjo, A.; Lim, H. K.; Camara, A.; Sikka, G.; Lim, H. K.; Sohi, J.; Santhanam, L.; Soucy, K.; Tuday, E.; Baraban, E.; Ilic, M.; Gerstenblith, G.; Nyhan, D.; Shoukas, A.; Christianson, D. W.; Alp, N. J.; Champion, H. C.; Huso, D.; Berkowitz, D. E. Endothelial arginase II. A novel target for the treatment of atherosclerosis. *Circ. Res.* **2008**, *102*, 923–932.
- (17) (a) Singh, R.; Pervin, S.; Karimi, A.; Cederbaum, S.; Chaudhuri, G. Arginase activity in human breast cancer cell lines: N ω -hydroxy-L-arginine selectively inhibits cell proliferation and induces apoptosis in MDA-MB-468 cells. *Cancer Res.* **2000**, *60*, 3305–3312. (b) Chang, C.-I.; Liao, J. C.; Kuo, L. Macrophage arginase promotes tumor cell growth and suppresses nitric oxide-mediated tumor cytotoxicity. *Cancer Res.* **2001**, *61*, 1100–1106. (c) Lind, S. D. Arginine and cancer. *J. Nutr.* **2004**, *134*, 2837S–2841S. (d) Bronte, V.; Zanovello, P. Regulation of immune responses by L-arginine metabolism. *Nat. Rev. Immunol.* **2005**, *5*, 641–654. (e) Zea, A. H.; Rodriguez, P. C.; Atkins, M. B.; Hernandez, C.; Signoretti, S.; Zabaleta, J.; McDermott, D.; Quiceno, D.; Youmans, A.; O'Neill, A.; Mier, J.; Ochoa, A. C. Arginase-producing myeloid suppressor cells in renal cell carcinoma patients: a mechanism of tumor evasion. *Cancer Res.* **2005**, *65*, 3044–3048. (f) Ochoa, A. C.; Zea, A. H.; Hernandez, C.; Rodriguez, P. C. Arginase, prostaglandins, and myeloid-derived suppressor cells in renal cell carcinoma. *Clin. Cancer Res.* **2007**, *13*, 721s–726s. (g) Marx, J. Cancer's bulwark against immune attack: MDS cells. *Science* **2008**, *319*, 154–156.
- (18) Baggio, R.; Elbam, D.; Kanyo, Z. F.; Carroll, P. J.; Cavalli, R. C.; Ash, D. E.; Christianson, D. W. Inhibition of Mn²⁺-arginase by borate leads to the design of a transition state analog inhibitor, 2(S)-amino-6-boronoheptanoic acid. *J. Am. Chem. Soc.* **1997**, *119*, 8107–8108.
- (19) Di Costanzo, L.; Sabio, G.; Mora, A.; Rodriguez, P. C.; Ochoa, A. C.; Centeno, F.; Christianson, D. W. Crystal structure of human arginase I at 1.29-Å resolution and exploration of inhibition in the immune response. *Proc. Natl. Acad. Sci. U.S.A.* **2005**, *102*, 13058–13063.
- (20) Di Costanzo, L.; Flores, L. V., Jr.; Christianson, D. W. Stereochemistry of guanidine-metal interactions: implications for L-arginine–metal interactions in protein structure and function. *Proteins* **2006**, *65*, 637–642.
- (21) Creighton, T. E. *Proteins: Structures and Molecular Properties*; W. H. Freeman: New York, 1992.
- (22) Storey, B. T.; Sullivan, W. W.; Moyer, C. L. The pK_a values of some 2-amino imidazolium ions. *J. Org. Chem.* **1964**, *29*, 3118–3120.
- (23) Sullivan, J. D.; Giles, R. L.; Looper, R. E. 2-Aminoimidazoles from Leucetta sponges: synthesis and biology of an important pharmacophore. *Curr. Bioact. Compd.* **2009**, *5*, 39–78.
- (24) (a) Mourabit, A. A.; Potier, P. Sponge's molecular diversity through the ambivalent reactivity of 2-aminoimidazole: a universal chemical pathway to the oroidin-based pyrrole-imidazole alkaloids and their palau'amine congeners. *Eur. J. Org. Chem.* **2001**, *2*, 237–243. (b) Hoffmann, H.; Lindel, T. Synthesis of the pyrrole-imidazole alkaloids. *Synthesis* **2003**, *12*, 1753–1783. (c) Rogers, S. A.; Bero, J. D.; Melander, C. Chemical synthesis and biological screening of 2-aminoimidazole-based bacterial and fungal antibiofilm agents. *ChemBioChem* **2010**, *11*, 396–410.
- (25) (a) Benoit-Vical, F.; Salery, M.; Soh, P. N.; Ahond, A.; Poupat, C. Girolline: a potential lead structure for antiplasmodial drug

- research. *Planta Med.* **2008**, *74*, 438–444. (b) Mancini, I.; Guella, G.; Debitus, C.; Waikedre, J.; Pietra, F. From inactive nortopsentin D, a novel bis(indole) alkaloid isolated from the axinellid sponge *Dragmacidon* sp. from deep waters south of New Caledonia, to a strongly cytotoxic derivative. *Helv. Chim. Acta* **1996**, *79*, 2075–2082.
- (26) Nagai, W.; Kirk, K. L.; Cohen, L. A. Synthesis of 2-amino-L-histidine and 2-aminohistamine. *J. Org. Chem.* **1973**, *38*, 1971–1974.
- (27) Friedel, M.; Lindel, T. Synthesis of L-aminohomohistidine (L-Ahh). *Tetrahedron Lett.* **2004**, *45*, 2779–2781.
- (28) Ulhaq, S.; Chinje, E. C.; Naylor, M. A.; Jaffar, M.; Stratford, I. J.; Threadgill, M. D. S-2-Amino-5-azolylpentanoic acids related to L-ornithine as inhibitors of the isoforms of nitric oxide synthase (NOS). *Bioorg. Med. Chem.* **1998**, *6*, 2139–2149.
- (29) (a) Zakharian, T. Y.; Di Costanzo, L.; Christianson, D. W. Synthesis of (2S)-2-amino-7,8-epoxyoctanoic acid and structure of its metal-bridging complex with human arginase I. *Org. Biomol. Chem.* **2008**, *6*, 3240–3243. (b) Zakharian, T. Y.; Di Costanzo, L.; Christianson, D. W. (S)-2-Amino-6-nitrohexanoic acid binds to human arginase I through multiple nitro-metal coordination interactions in the binuclear manganese cluster. *J. Am. Chem. Soc.* **2008**, *130*, 17254–17255.
- (30) Adamczyk, M.; Johnson, D. D.; Reddy, R. E. Collagen crosslinks: a convenient synthesis of *tert*-butyl-(2S)-2-[(*tert*-butoxycarbonyl)-amino]-4-(2-oxiranyl)butanoate. *Tetrahedron: Asymmetry* **1999**, *10*, 775–781.
- (31) Ulhaq, S.; Naylor, M. A.; Chinje, E. C.; Threadgill, M. D.; Stratford, I. J. S-2-Amino-5-(2-nitroimidazol-1-yl)pentanoic acid: a model for potential bioreductively activated prodrugs for inhibitors of nitric oxide synthase (NOS) activity. *Anti-Cancer Drug Des.* **1997**, *12*, 61–65.
- (32) Cama, E.; Shin, H.; Christianson, D. W. Design of amino acid sulfonamides as transition-state analogue inhibitors of arginase. *J. Am. Chem. Soc.* **2003**, *125*, 13052–13057.
- (33) Ciapetti, P.; Falorni, M.; Mann, A.; Taddei, M. 2-Amino-4-bromobutanoic acid. A versatile reagent for the synthesis of nonnatural amino acids. *Molecules Online* **1998**, *2*, 86–93.
- (34) Rüegg, U. T.; Russell, A. S. A rapid and sensitive assay for arginase. *Anal. Biochem.* **1980**, *102*, 206–212.
- (35) Pearson, J. T.; Hill, J. J.; Swank, J.; Isoherranen, N.; Kunze, K. L.; Atkins, W. M. Surface plasmon resonance analysis of antifungal azoles binding to CYP3A4 with kinetic resolution of multiple binding orientations. *Biochemistry* **2006**, *45*, 6341–6353.
- (36) Lancini, G. C.; Lazzari, E. A new synthesis of alkyl and aryl 2-aminoimidazoles. *J. Heterocycl. Chem.* **1966**, *3*, 152–154.
- (37) (a) Alberti, G.; Bertini, I.; Luchinat, C.; Scozzafava, A. A new class of inhibitors capable of binding both the acidic and alkaline forms of carbonic anhydrase. *Biochim. Biophys. Acta* **1981**, *668*, 16–26. (b) Bertini, I.; Luchinat, C. Cobalt(II) as a probe of the structure and function of carbonic anhydrase. *Acc. Chem. Res.* **1983**, *16*, 272–279.
- (38) Kannan, K. K.; Chakravarty, S.; Satyamurthy, P.; Ramanadham, M.; Kumar, V.; Yadav, V. S. Structure and function of carbonic anhydrase: Synchrotron X-ray diffraction studies of human carbonic anhydrase I and inhibitor complexes. *Synchrotron Radiat. Biosci.* **1994**, *86*–95.
- (39) Mangani, S.; Liljas, A. Crystal structure of the complex between human carbonic anhydrase II and the aromatic inhibitor 1,2,4-triazole. *J. Mol. Biol.* **1993**, *232*, 9–14.
- (40) Marino, J. P., Jr.; Fisher, P. W.; Hofmann, G. A.; Kirkpatrick, R. B.; Janson, C. A.; Johnson, R. K.; Ma, C.; Mattern, M.; Meek, T. D.; Ryan, M. D.; Schulz, C.; Smith, W. W.; Tew, D. G.; Tomazek, T. A., Jr.; Veber, D. F.; Xiong, W. C.; Yamamoto, Y.; Yamashita, K.; Yang, G.; Thompson, S. K. Highly potent inhibitors of methionine aminopeptidase-2 based on a 1,2,4-triazole pharmacophore. *J. Med. Chem.* **2007**, *50*, 3777–3785.
- (41) Rahman, M. N.; Vlahakis, J. Z.; Szarek, W. A.; Nakatsu, K.; Jia, Z. X-ray crystal structure of human heme oxygenase-1 in complex with 1-(adamantan-1-yl)-2-(1H-imidazol-1-yl)ethanone: a common binding mode for imidazole-based heme oxygenase-1 inhibitors. *J. Med. Chem.* **2008**, *51*, 5943–5952.
- (42) Berka, V.; Palmer, G.; Chen, P.-F.; Tsai, A.-L. Effects of various imidazole ligands on heme conformation in endothelial nitric oxide synthase. *Biochemistry* **1998**, *37*, 6136–6144.
- (43) (a) Kenyon, N. J.; Bratt, J. M.; Linderholm, A. L.; Last, M. S.; Last, J. A. Arginases I and II in lungs of ovalbumin-sensitized mice exposed to ovalbumin: sources and consequences. *Toxicol. Appl. Pharmacol.* **2008**, *230*, 269–275. (b) Bratt, J. M.; Franzi, L. M.; Linderholm, A. L.; Last, M. S.; Kenyon, N. J.; Last, J. A. Arginase enzymes in isolated airways from normal and nitric oxide synthase 2-knockout mice exposed to ovalbumin. *Toxicol. Appl. Pharmacol.* **2009**, *234*, 273–280.
- (44) Custot, J.; Moali, C.; Brollo, M.; Boucher, J. L.; Delaforge, M.; Mansuy, D.; Tenu, J. P.; Zimmermann, J. L. The new α -amino acid N^{ω} -hydroxy-nor-L-arginine: a high-affinity inhibitor of arginase well adapted to bind to its manganese cluster. *J. Am. Chem. Soc.* **1997**, *119*, 4086–4087.
- (45) Custot, J.; Boucher, J.-L.; Vadon, S.; Guedes, C.; Dijols, S.; Delaforge, M.; Mansuy, D. N^{ω} -Hydroxyamino- α -amino acids as a new class of very strong inhibitors of arginases. *J. Biol. Inorg. Chem.* **1996**, *1*, 73–82.
- (46) Di Costanzo, L.; Moulin, M.; Haertlein, M.; Meilleur, F.; Christianson, D. W. Expression, purification, assay, and crystal structure of perdeuterated human arginase I. *Arch. Biochem. Biophys.* **2007**, *465*, 82–89.
- (47) Schuck, P. Use of surface plasmon resonance to probe the equilibrium and dynamic aspects of interactions between biological macromolecules. *Annu. Rev. Biophys. Biomol. Struct.* **1997**, *26*, 541–566.
- (48) Otwinowski, Z.; Minor, W. Processing of X-ray diffraction data collected in oscillation mode. *Methods Enzymol.* **1997**, *276*, 307–326.
- (49) Di Costanzo, L.; Pique, M. E.; Christianson, D. W. Crystal structure of human arginase I complexed with thiosemicarbazide reveals an unusual thiocarbonyl μ -sulfide ligand in the binuclear manganese cluster. *J. Am. Chem. Soc.* **2007**, *129*, 6388–6389.
- (50) Yeates, T. O. Detecting and overcoming crystal twinning. *Methods Enzymol.* **1997**, *276*, 344–358.
- (51) McCoy, A. J.; Grosse-Kunstleve, R. W.; Adams, P. D.; Winn, M. D.; Storoni, L. C.; Read, R. Phaser crystallographic software. *J. Appl. Crystallogr.* **2007**, *40*, 658–674.
- (52) Brünger, A. T.; Adams, P. D.; Clore, G. M.; DeLano, W. L.; Gros, P.; Grosse-Kunstleve, R. W.; Jiang, J. S.; Kuszewski, J.; Nilges, M.; Pannu, N. S.; Read, R. J.; Rice, L. M.; Simonson, T.; Warren, G. L. Crystallography & NMR system: a new software suite for macromolecular structure determination. *Acta Crystallogr. D* **1998**, *54*, 905–921.
- (53) Sheldrick, G. M. A short history of SHELX. *Acta Crystallogr. A* **2008**, *64*, 112–122.
- (54) Laskowski, R. A.; MacArthur, M. W.; Moss, D. S.; Thornton, J. M. PROCHECK: a program to check the stereochemical quality of protein structures. *J. Appl. Crystallogr.* **1993**, *26*, 283–291.